High Power Laser Science and Engineering, (2024), Vol. 12, e34, 6 pages.
doi:10.1017/hpl.2024.15

HIGH POWER LASER SCIENCE AND ENGINEERING

RESEARCH ARTICLE

Random pinhole attenuator for high-power laser beams

Seong Cheol Park[1,2], Hyeok Yun[2,3], Jin Woo Yoon[2,3], Seong Ku Lee[2,3], Jae Hee Sung[2,3], Il Woo Choi[2,3], Chang Hee Nam[1,2], and Kyung Taec Kim[1,2]

[1] *Department of Physics and Photon Science, Gwangju Institute of Science and Technology, Gwangju, Republic of Korea*

[2] *Center for Relativistic Laser Science, Institute for Basic Science, Gwangju, Republic of Korea*

[3] *Advanced Photonics Research Institute, Gwangju Institute of Science and Technology, Gwangju, Republic of Korea*

(Received 14 December 2023; revised 5 February 2024; accepted 7 March 2024)

Abstract

The intensity attenuation of a high-power laser is a frequent task in the measurements of optical science. Laser intensity can be attenuated by inserting an optical element, such as a partial reflector, polarizer or absorption filter. These devices are, however, not always easily applicable, especially in the case of ultra-high-power lasers, because they can alter the characteristics of a laser beam or become easily damaged. In this study, we demonstrated that the intensity of a laser beam could be effectively attenuated using a random pinhole attenuator (RPA), a device with randomly distributed pinholes, without changing the beam properties. With this device, a multi-PW laser beam was successfully attenuated and the focused beam profile was measured without any alterations of its characteristics. In addition, it was confirmed that the temporal profile of a laser pulse, including the spectral phase, was preserved. Consequently, the RPA possesses significant potential for a wide range of applications.

Keywords: high-power laser; intensity attenuation; laser diagnostics

1. Introduction

The intensity adjustment of a laser beam is commonly required in optics experiments to avoid the damage of optical components. The intensity of the laser beam can be adjusted using an optical device, such as a partial reflector, polarizing plate or absorption filter[1,2]. In most applications, such a device can be inserted to adjust the intensity of a laser beam[3]. In some cases the intensity adjustment, however, becomes a challenging task in order not to alter the laser characteristics. One example is the beam profile measurement after a plasma mirror, used to enhance the temporal contrast of an ultra-high-intensity laser[4,5]. Since the plasma mirror works at very high intensity, the laser intensity cannot be attenuated before the plasma mirror. The insertion of a partial reflection mirror without changing the beam alignment cannot be easily done due to the large beam size of such a laser. For example, the 4 PW laser at the Center for Relativistic Laser Science (CoReLS) has the beam size of 30 cm[6,7]. It is also difficult to add a polarizing plate or an absorption filter due to optical damage, wavefront deformation and additional dispersion. Consequently, there is a practical need for a new approach capable of adjusting the intensity of a high-power laser without modifying the laser characteristics.

As another example, a case of measuring the temporal profile of a laser pulse can be considered. The temporal profile of the laser pulse can be measured using various pulse characterization techniques. These techniques rely on nonlinear processes such as second harmonic generation or ionization. For example, the tunneling ionization with a perturbation for the time-domain observation of an electric field (TIPTOE) method relies on the nonlinearity of ionization for the temporal characterization[8,9], which is highly sensitive to the intensity of the laser pulse. Thus, it is essential to adjust the intensity of the laser beam precisely. Since devices such as variable neutral density (ND) filters alter the dispersion condition of the laser pulse, the temporal profile of the laser beam is changed[10]. Therefore, a new approach for attenuating the intensity of the laser beam is also required.

In this work, we demonstrated the attenuation of laser intensity without changing the properties of a high-power laser beam using a random pinhole attenuator (RPA). The RPA is a board with a large number of randomly distributed pinholes. This kind of device has been utilized for an X-ray beam[11]. The beam profile of the CoReLS 4 PW laser

Correspondence to: Kyung Taec Kim, Center for Relativistic Laser Science, Institute for Basic Science, Gwangju 61005, Republic of Korea. Email: kyungtaec@gist.ac.kr

was measured using the RPA. We demonstrated also the continuous attenuation of laser intensity using the RPA with the gradient in the pinhole number density. In addition, the RPA was applied for the temporal characterization of ultra-high-intensity laser pulses because it does not introduce additional dispersion. Since the RPA can be generally used to adjust the intensity of the laser beam, it will be highly useful in many optical applications.

2. Theory of the random pinhole attenuator

An RPA has been designed with the following basic idea. A laser beam with flat-top intensity, characterized by a beam diameter D, is considered to be focused using an ideal lens, as shown in Figure 1(a). Assuming a constant intensity before the lens, the beam energy is proportional to D^2 and the size of the beam at the focus is proportional to D^{-2}. Thus, the intensity at the focus is proportional to D^4. In the same way, the intensity of the laser beam, diffracted through a pinhole, is proportional to d^4. If we introduce N pinholes into this scenario, the strength of the electric field at the focal point would be enhanced by N times, leading to an overall intensity increase of N^2. Therefore, the attenuation factor of the beam intensity (i.e., the intensity ratio with and without the pinholes) can be obtained as $\left(N^2 d^4\right)/D^4$[12].

It should be noted that this attenuation factor is obtained based on the ordinary Kirchhoff diffraction theory. When the size of the hole becomes comparable to the laser wavelength, other effects, such as plasmonic and waveguide effects, may arise depending on the material and the thickness of the RPA[13,14]. These effects are ignored because the pinhole diameters are much larger than the laser wavelength in this work.

With a sufficiently large number of pinholes, the shape of the focused beam can be maintained as it would be in the absence of pinholes. However, a uniformly distributed array of pinholes results in the appearance of diffracted laser beams on the focal plane, in addition to the laser beam's focus. Other laser beams created by the higher-order diffraction can be eliminated by randomizing the distribution of the pinholes. In such a setup, all laser beams on the focal plane, with the exception of the zeroth-order diffraction, are transformed into noise, thereby avoiding the issue of unwanted diffraction.

Figure 1 provides a simplified illustration of light propagation. The passage of light through a board punctuated by randomly distributed pinholes is illustrated in Figure 1(a). The calculated light propagation on the yz-plane shown in Figure 1(a) is shown in Figure 1(b). We assumed that the laser beam with a diameter of 13 mm is focused using a 1 m focal length ideal lens. The pinhole diameter is 60 μm. The number of pinholes is 1000. The light diffracted through each pinhole is gathered to a single focal point. Since the optical path lengths from each pinhole to the focus are the same, the beam shape is not changed from the original beam shape. However, their optical path lengths vary depending on the position of the pinhole for the higher-order diffractions, and their phases are randomized due to the random positions of the pinholes. These beams do not form a well-defined beam, but contribute to the background noise.

To use the RPA, the signal-to-noise ratio (SNR) should be sufficiently high. The energy of the laser beam diffracted through a single pinhole is proportional to d^2, which is diffracted in an area proportional to $(\lambda f/d)^2$. For the N beams transmitted through the random pinholes, the averaged beam intensity at the focal plane will be proportional to $\left(Nd^4\right)/(\lambda f)^2$. Consequently, the noise intensity is proportional to the number of pinholes N, while the intensity of the zeroth-order focused beam is proportional to N^2. Therefore, the SNR is proportional to N[15]. The greater the number of pinholes, the higher the SNR becomes.

We made a series of calculations to estimate the SNR with different number densities of pinholes, as shown in Figure 1(c). It is clearly shown that the SNR is enhanced by increasing the number of pinholes for the same beam diameter. Upon calculations with 1000, 3000 and 10,000 pinholes, there is a discernible trend of improving SNR with the increasing number of pinholes.

For an experimental demonstration, an RPA with a density gradient is fabricated by etching holes through a thin metal foil. The pinholes should be randomly distributed with a uniform number density. Also, they must be well separated

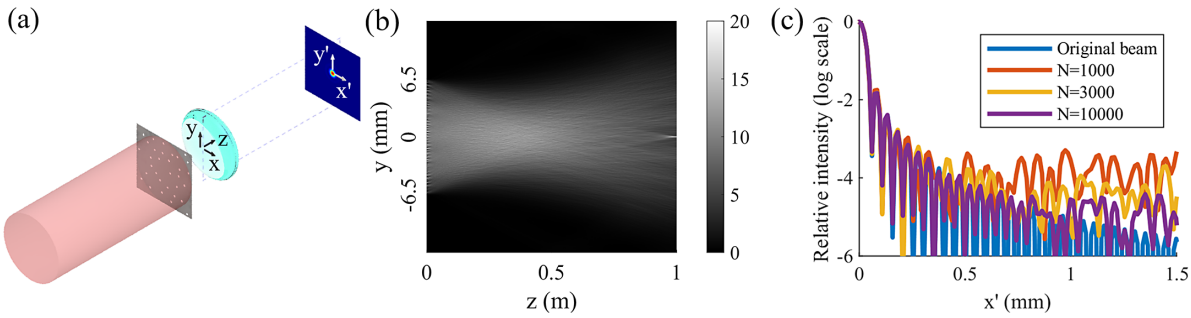

Figure 1. Attenuation of laser intensity using a random pinhole attenuator (RPA). (a) Schematic diagram for attenuating the laser intensity using the RPA. (b) Intensity of the laser beam on the yz-plane shown in (a). (c) Intensity distribution at the focal plane calculated for different numbers of pinholes.

https://doi.org/10.1017/hpl.2024.15 Published online by Cambridge University Press

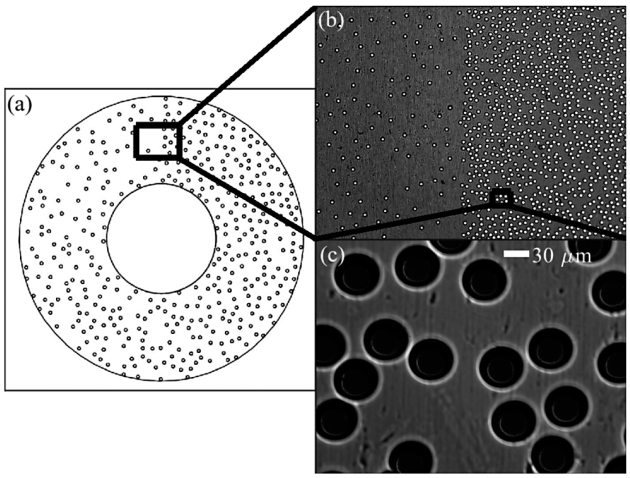

Figure 2. Random pinhole array fabricated with a number-density gradient. (a) Simplified model of the random pinhole array. (b), (c) Microscope images of the random pinhole array obtained with (b) 20× and (c) 50× magnification.

for fabrication. In order to satisfy these conditions, we used the Poisson disc sampling algorithm[16,17]. The density of the pinhole varies from 112 to 11 holes/mm^2, which corresponds to an optical density (OD) from 2 to 4. Here, the OD value represents the intensity ratio of the laser beam obtained at the focus with and without the random pinhole array. Thus, the OD of 2 means that the beam intensity is reduced to 1/100 of the original value obtained without the random pinhole array.

As illustrated in Figure 2(a), the RPA was designed to adjust the OD values by angle rotation as in a commercial variable ND filter (for example, a Thorlabs NDC-100C-4M). The number density of the pinholes gradually increases along the angular direction. Figure 2(b) shows an image captured using a 20× magnification microscope lens, which includes both the maximum and minimum densities of holes on the board. Figure 2(c) shows the employment of a 50× magnification microscope lens. We made circular pinholes. The hole diameter is 30 μm. The shape of the pinhole affects the shape of the diffracted beam. However, the focused beam is much smaller than the diffracted beam of the individual pinhole. Therefore, the shape of the individual pinhole is not critical.

To verify the idea of an RPA, we first measured the beam profile using an ND filter (Thorlabs, NDC-100C-4M) and, after that, the beam profile was measured using the RPA. A 633 nm diode laser was used for this experiment. A lens with the focal length of 600 mm was utilized to focus the beam, and its profile at the focus was imaged using a complementary metal–oxide–semiconductor (CMOS) camera (pco.edge 5.5, 16-bit sCMOS camera). The intensity profiles of the laser beam are shown in Figures 3(a) and 3(b), indicating a good agreement. Consequently, it can be concluded that the beam profile can be measured with the insertion of the random pinhole board. Also, we measured the OD values, showing that the actual OD value varies from 2 to 3.89, as shown in Figure 3(f). Since the RPA does not change the property of the laser beam, it offers an easy way to control the laser beam intensity.

3. Attenuation of a PW laser beam

To demonstrate the intensity attenuation of a high-power laser beam, we used the CoReLS 4 PW laser. The CoReLS 4 PW laser was operated with an energy of 80 J before the

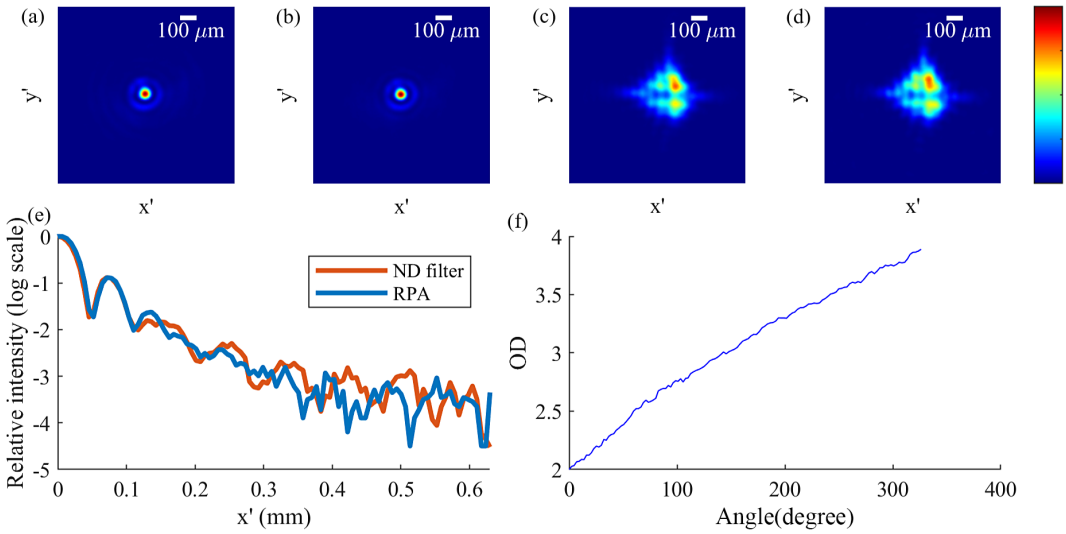

Figure 3. Beam profiles of the focused beam. (a)–(d) The beam profiles of the focused beam and the distorted beam. The intensity is attenuated using (a), (c) an ND filter (Thorlabs NDC-100C-4M) and (b), (d) a random pinhole attenuator (RPA). (e) The intensity lineouts along the *x*-axis of the beam shown in (a) and (b). The *x*-axis represents the distance from the beam's center, while the *y*-axis depicts the relative intensity on a logarithmic scale. (f) The measured optical density versus the angle of the variable attenuation board. OD denotes the optical density.

https://doi.org/10.1017/hpl.2024.15 Published online by Cambridge University Press

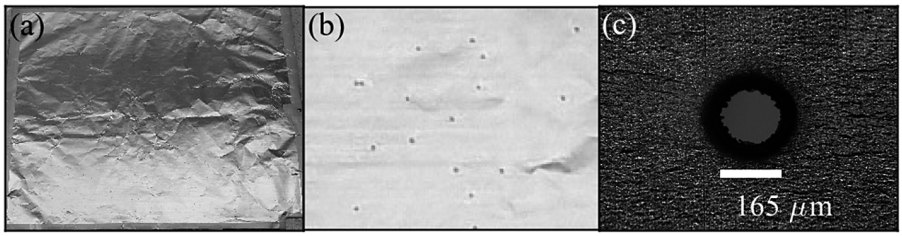

Figure 4. Photos of an RPA. (a) RPA fabricated on an aluminum foil by laser drilling. (b) Magnified image showing randomly distributed pinholes. (c) Image of a pinhole.

grating compressor. It has been used for various applications, such as relativistic high harmonic generation, laser wake field acceleration[18] and proton acceleration[19]. In these applications, maintaining an exceptional temporal contrast between pre-pulses and the main pulse is critical. Therefore, the CoReLS 4 PW laser operates with double plasma mirrors[20]. It suppresses the intensity of the pre-pulses while the main pulse is reflected with a high reflectance. Since the plasma mirror works when the laser power is sufficiently high, we could not reduce the laser intensity before the plasma mirror. Thus, it was difficult to measure the beam profile of the laser beam at the focus because the conventional techniques to attenuate the beam intensity could not be applied due to the large beam size (30 cm).

We fabricated an RPA to accommodate the large beam of the CoReLS 4 PW laser, as shown in Figure 4. The detailed parameters of the laser system, including the near-field beam shape, are explained in Ref. [20]. The random pinhole board was made with 2500 pinholes with an aperture diameter of 165 μm, as shown in Figure 4(c). These pinholes, distributed randomly within a 300-mm circle corresponding to the laser beam's diameter, were fabricated using an aluminum foil whose thickness is 15 μm, as shown in Figure 4(a). The flatness of the foil does not affect the shape of the focused beam. The pinholes were made by laser drilling using a mJ class, 1 kHz repetition rate, 30 fs pulse duration, 800 nm wavelength Ti:sapphire laser, as shown in Figure 4(b). The energy density of the laser beam that falls on the RPA was 37 mJ/cm^2, which is well below the damage threshold of the aluminum foil[21]. No damage was observed after many laser shots.

The PW laser beam is focused using an off-axis parabola with a 550 mm focal length. Since the laser beam intensity is sufficiently reduced, we could measure it directly using an ordinary 12-bit charge-coupled device (CCD) camera, as shown in Figures 5(a) and 5(b). We first measured the beam profile with a commercial ND filter when the laser intensity was weak, as shown in Figure 5(a). We reduced the beam energy down to 4 J. Then, the laser beam was reflected using two 1% reflection mirrors. We also used a waveplate to reduce the laser intensity to 3%. In this case, the plasma mirror was not used. Thus, the laser beam energy was about 10 μJ. Its beam profile is shown in Figure 5(a).

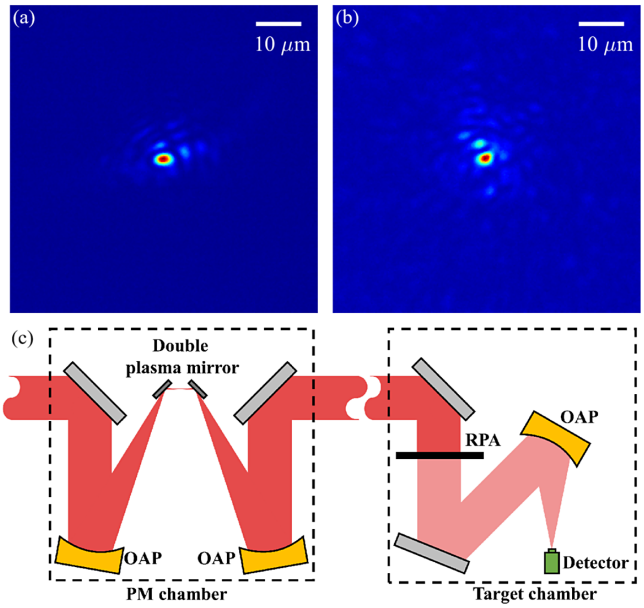

Figure 5. Beam profiles of the CoReLS 4 PW laser. (a) Beam profile of the focused 10-μJ laser beam without passing through the plasma mirror system and (b) beam profile of the focused laser beam obtained with the plasma mirror system. The energy of the laser beam was 80 J before the grating pulse compressor. (c) The schematics of the CoReLS 4 PW laser. The plasma mirrors (PMs), RPA and off-axis parabola (OAP) are shown.

After that, the laser beam energy was increased to the maximum value (80 J) without having any other attenuation before the plasma mirror. Then, the plasma mirrors were used. The random pinhole board can be positioned at any place in the beam path after the plasma mirror but before the focusing mirror. We placed it about 1 m before the focusing mirror, as shown in Figure 5(c). The beam profile of the laser beam at the focus with the pulse energy of 80 J, which is measured before the compressor[6], is shown in Figure 5(b).

A noticeable difference exists between the beam profiles in Figures 5(a) and 5(b), attributable to the plasma mirror's deployment. Specifically, in Figure 5(a), the energy insufficiency prevents plasma generation from the mirror, while in Figure 5(b), the laser beam is reflected off the plasma, given its full energy utilization. The observable non-convergence of the full power beam shown in Figure 5(b) suggests that the optimization condition of an adaptive optic

https://doi.org/10.1017/hpl.2024.15 Published online by Cambridge University Press

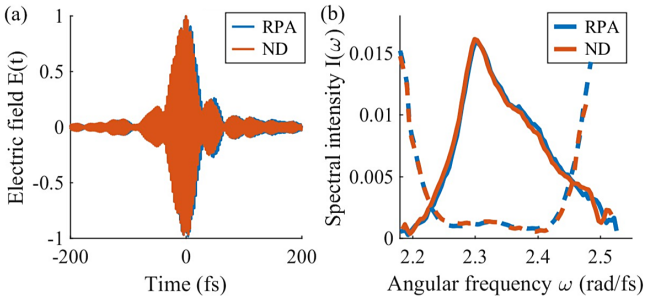

Figure 6. Comparison of temporal characteristics of two attenuation cases. (a) Laser electric fields obtained with an ND filter (red line) and with an RPA (blue line). (b) Spectral intensities and phases of the two cases.

system (i.e., wavefront sensor and deformable mirror) found for the low-intensity beam would not be the best condition for the high-power laser beam.

4. Attenuation of a laser beam for pulse characterization

The advantage of attenuating the laser beam intensity using the random pinhole board is that it does not alter the property of the laser beam. This is also a great advantage for the temporal characterization of an ultrashort laser pulse. We employed the TIPTOE pulse characterization technique to demonstrate that the laser pulse can be measured without imposing additional dispersion. The temporal profile of the laser beam is measured from the modulation of the ionization yield, which is highly sensitive to the laser intensity. Thus, the use of the correct intensity is critical in this measurement.

The temporal profiles were measured under two conditions. Firstly, the intensity of the laser beam was attenuated by a commercial variable ND filter (Thorlabs, NDC-100C-4M) and the temporal profile of the laser pulse was measured. Then, the temporal profile was also measured using the RPA, as shown in Figure 2. For the latter measurement, an ND filter with the OD of 0.04 was inserted to measure the laser pulse with the same dispersion condition.

The temporal profiles are compared in Figure 6(a). The spectrum and spectral phases are compared in Figure 6(b). They show a good agreement, indicating that the RPA does not impose any additional dispersion on the laser pulse. It should be noted that the attenuation factor is not dependent on the wavelength. Thus, it can be used for a broadband laser pulse. We also checked the polarization state of the laser beam before and after the RPA. The polarization state was not changed. Therefore, the RPA can be used for the pulse measurement without changing the alignment, polarization or dispersion condition.

5. Conclusions

We demonstrated the attenuation of laser intensity using an RPA without changing the properties of a high-power laser beam, such as alignment, polarization and dispersion. Firstly, we provided a theoretical framework illustrating the capability of the RPA. Our calculation showed that the RPA does not significantly alter the beam profile of the focus, which was verified by measuring the beam profile of a diode laser at the focal point. More importantly, we confirmed its usefulness by measuring the beam profile of the CoReLS 4 PW laser, especially after a plasma mirror. In addition, it was verified using the TIPTOE technique that the dispersion condition of a laser beam remained the same after the application of an RPA.

The ability to measure the beam profile of a high-power laser system at full power is critical in many applications. Given the challenges associated with measuring the focus under full-energy conditions within such systems, our experimental findings mitigate a prevalent uncertainty in application experiments. Importantly, the consistent characteristics of the attenuated beam extend its utility across diverse applications. Since it does not affect the spatial and temporal property of the laser beam, it will also useful for the measurement of spatio-temporal coupling[22,23]. In addition, the RPA can be easily fabricated by chemical etching or laser drilling. Thus, it will be practically useful in many applications.

Acknowledgement

This work was supported by an Institute for Basic Science grant (IBS-R012-D1) and a National Research Foundation of Korea (NRF) grant funded by the Korea government (MIST) (No. 2022R1A2C3006025 and No. RS-2023-00218180).

References

1. H. A. Macleod, *Thin-Film Optical Filters* (CRC Press, 2017).
2. M. Banning, J. Opt. Soc. Am. **37**, 686 (1947).
3. C. B. Roundy and K. Kirkham, in *Laser Beam Shaping* (CRC Press, 2014), p. 463.
4. H. C. Kapteyn, M. M. Murnane, A. Szoke, and R. W. Falcone, Opt. Lett. **16**, 490 (1991).
5. A. Lévy, T. Ceccotti, P. D'Oliveira, F. Réau, M. Perdrix, F. Quéré, P. Monot, M. Bougeard, H. Lagadec, and P. Martin, Opt. Lett. **32**, 310 (2007).
6. J. H. Sung, H. W. Lee, J. Y. Yoo, J. W. Yoon, C. W. Lee, J. M. Yang, Y. J. Son, Y. H. Jang, S. K. Lee, and C. H. Nam, Opt. Lett. **42**, 2058 (2017).
7. J. W. Yoon, Y. G. Kim, I. W. Choi, J. H. Sung, H. W. Lee, S. K. Lee, and C. H. Nam, Optica **8**, 630 (2021).
8. S. B. Park, K. Kim, W. Cho, S. I. Hwang, I. Ivanov, C. H. Nam, and K. T. Kim, Optica **5**, 402 (2018).
9. W. Cho, S. I. Hwang, C. H. Nam, M. R. Bionta, P. Lassonde, B. E. Schmidt, H. Ibrahim, F. Légaré, and K. T. Kim, Sci. Rep. **9**, 16067 (2019).
10. E. Hecht, *Optics* (Pearson, 2016).
11. J. M. Wengrowicz and G. Hurvitz, Appl. Opt. **59**, 3174 (2020).
12. B. E. Saleh and M. C. Teich, *Fundamentals of Photonics* (John Wiley & Sons, 2019).
13. H. A. Bethe, Phys. Rev. **66**, 163 (1944).

https://doi.org/10.1017/hpl.2024.15 Published online by Cambridge University Press

14. T. W. Ebbesen, H. J. Lezec, H. F. Ghaemi, T. Thio, and P. A. Wolff, Nature **391**, 667 (1998).
15. A. Sommerfeld, *Lectures on Theoretical Physics: Optics* (Academic Press, 1954), Vol. 4.
16. D. Dunbar and G. Humphreys, ACM Trans. Graphics **25**, 503 (2006).
17. R. Bridson, in *ACM SIGGRAPH 2007 Sketches* (2007), p. 22-es.
18. B. S. Rao, J. H. Jeon, H. T. Kim, and C. H. Nam, Plasma Phys. Control. Fusion **60**, 095002 (2018).
19. P. Wang, Z. Gong, S. G. Lee, Y. Shou, Y. Geng, C. Jeon, I. J. Kim, H. W. Lee, J. W. Yoon, and J. H. Sung, Phys. Rev. X **11**, 021049 (2021).
20. I. W. Choi, C. Jeon, S. G. Lee, S. Y. Kim, T. Y. Kim, I. J. Kim, H. W. Lee, J. W. Yoon, J. H. Sung, and S. K. Lee, Opt. Lett. **45**, 6342 (2020).
21. S. Xu, Y. Chen, H. Liu, X. Miao, X. Yuan, and X. Jiang, Optik **212**, 164628 (2020).
22. S. Akturk, X. Gu, P. Bowlan, and R. Trebino, J. Opt. **12**, 093001 (2010).
23. A. Jeandet, S. W. Jolly, A. Borot, B. Bussière, P. Dumont, J. Gautier, O. Gobert, J.-P. Goddet, A. Gonsalves, A. Irman, W. P. Leemans, R. Lopez-Martens, G. Mennerat, K. Nakamura, M. Ouillé, G. Pariente, M. Pittman, T. Püschel, F. Sanson, F. Sylla, C. Thaury, K. Zeil, and F. Quéré, Opt. Express **30**, 3262 (2022).

https://doi.org/10.1017/hpl.2024.15 Published online by Cambridge University Press